Study of dendritic growth of zinc crystals on the edges of steel sheet

L. N. Bengoa, S. Bruno, H. A. Lazzarino, P. R. Seré & W. A. Egli

Journal of Applied Electrochemistry

ISSN 0021-891X

J Appl Electrochem
DOI 10.1007/s10800-014-0722-y

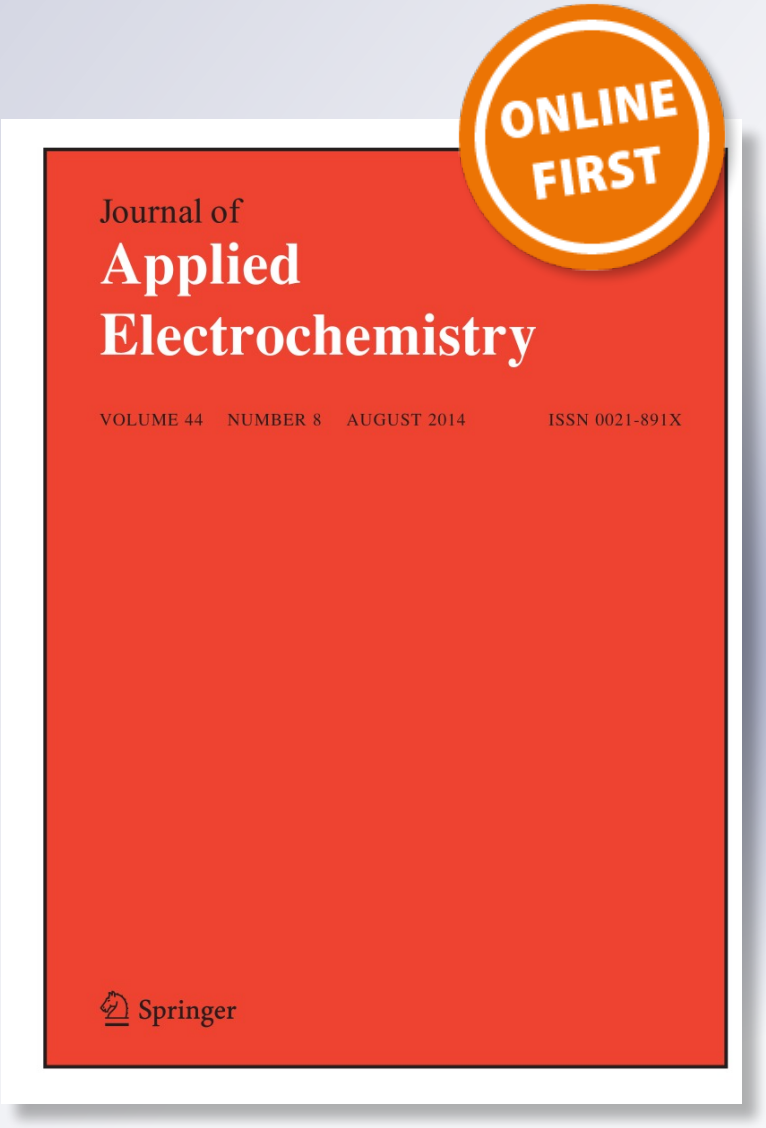

Springer

J Appl Electrochem
DOI 10.1007/s10800-014-0722-y

RESEARCH ARTICLE

Study of dendritic growth of zinc crystals on the edges of steel sheet

L. N. Bengoa · S. Bruno · H. A. Lazzarino · P. R. Seré · W. A. Egli

Received: 16 May 2014 / Accepted: 22 July 2014

Abstract In this paper, the formation of zinc dendrites at the strip edge of an industrial electrogalvanizing line was studied. For that purpose, a rotating washer electrode was designed to reproduce the hydrodynamic conditions and the current density distribution found in the industrial process. Polarization curves were recorded at different rotation speeds in order to investigate the electrokinetic behavior of the cathodic process. The induction time for dendritic growth was estimated for different overpotential values and the existence of a minimum overpotential below which dendrites do not grow was confirmed. Dendrite precursors on the edge of the washers were well characterized and its birth and precise location were studied. The general model of disperse and dendritic metal electrodeposit formation derived by Popov et al. was used to explain the effect of electrolyte zinc concentration, rotation speed of the cathode, electrolyte temperature and edge roughness on the size and morphology of dendrites. The results showed that this theory provides an accurate description of the phenomenon even for non-stationary electrodes, which have not been extensively studied so far. The experimental setup proved to be a powerful means to study the formation of dendritic growth of zinc crystals on the edges of steel strip and is well suited to characterize other metals that produce this type of defect.

Keywords Electroplating · Dendritic growth · Zinc · Galvanization

1 Introduction

Electrolytic deposition of metals on smooth flat cathode surfaces usually can be easily adjusted to produce homogeneous, non-porous and good quality coatings. When the object to be coated has rough surfaces or specific complicated shapes, some action has to be taken to avoid primary and secondary current distribution problems [1–3]. Localized zones with poor throwing power as corners and grooves may cause low coating thicknesses and high porosity. In contrast, protrusions, peaks and singular high points of the surface topography are usually overcoated, and sometimes present a completely different morphology from that of the flat surface, growing in a dendritic pattern. These topics are commonly found in batch electroplating of metals [4] and are usually well compensated with geometric considerations in anode design and also with the addition of the right additives (levelers and brighteners) [5–7]. One special case is the continuous production of electroplated steel strip in which the general electrolytic process conditions are designed and controlled in order to optimize the coating quality on the flat portion of the strip, leaving the edges as unavoidable singular points susceptible to current density (CD) distribution problems. The most common side effect is the growth of loosely adherent deposits, with either high surface roughness, low brightness or a different color in a narrow stripe near the edges of the

L. N. Bengoa (✉) · P. R. Seré · W. A. Egli
Center for Paints and Coatings Development (CICBA-CONICET), Av. 52 e/121 y 122, 1900 La Plata, Argentina
e-mail: leandrobengoa@gmail.com

L. N. Bengoa · P. R. Seré
Engineering School, National University of La Plata, Av.1 y 47, 1900 La Plata, Argentina

S. Bruno
REDE-AR, TenarisSiderca, 2804 Campana, Argentina

H. A. Lazzarino
Siderar, Ternium, 1888 Florencio Varela, Argentina

Published online: 12 August 2014

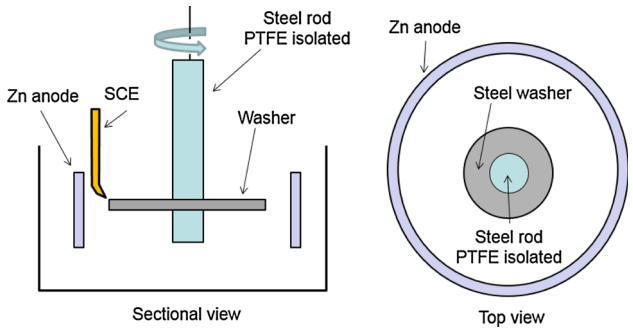

Fig. 1 Cell scheme for strip edge simulation

strip. Some examples of this problem are the white edge defect in tinplate production (causing quality rejections), the appearance of yellow edges during Cr plating in tin free steel, and the generation of large poor adherent dendrite crystals during Zn deposition in electrogalvanized steel, which causes dents during stamping in automotive industry [8–11]. One way to compensate these problems is the installation of automatic edge masks in the production lines, physically shielding the edges of the strip with a dielectric. The latter involves important investment and maintenance costs and considerable operating problems. In general, these quality defects seen on the final product are the visual macroscopic evidence of a microscopic process: metal deposition and dendrite formation [12]. This type of crystal growth has been widely studied in the last decades [13–16] and in recent years a well-structured and complete theory has been presented [17]. All these studies have been done in well-established and controlled static conditions that are quite different from those found in industrial processes and particularly at the edges of the steel strip in real production lines. In order to know how the process variables affects the generation and growth of this type of undesired metal deposits we have designed a new rotating washer electrode (RWE) that reproduces the hydrodynamic and current distribution of the strip edge usually found in industrial layouts. In this work, we present some basic results for zinc electrodeposition on steel cathodes.

2 Experimental

2.1 Rotating washer electrode (RWE)

To simulate the fluid dynamic conditions and the current distribution at the steel strip edge during the continuous electrogalvanizing process, a novel rotating system was designed with the geometry indicated in Fig. 1. This system shows the steel washer edge continuously moving in one direction facing a zinc anode. This resembles the geometry of the strip edge usually found in a production line. The washer cathode (with 8 mm inner diameter and 40 mm outer diameter) was made from 0.7 mm thickness SAE 1010 steel strip, cut with a high precision automatic laser-cutting machine. These washers were mounted on a steel rod isolated with a Teflon cylinder, leaving an exposed area of 0.194 dm^2. Electrical contact between the washer cathode and the steel rod was assured with a steel nut. A 70 mm internal diameter ring of pure zinc ingot was cast and used as anode [8–10].

Table 1 Summary of experimental conditions

	Minimum value	Maximum value
Washer rotation speed (ω)	400 rpm	1200 rpm
Zinc concentration (Zn^{+2})	40 g/L	140 g/L
Solution temperature (T)	40 °C	70 °C
Current density (CD)	20 A/dm^2	65 A/dm^2
Overpotential (η)	3.8 V	5.3 V

Washer rotation speed (ω) was varied between 400 and 1200 rpm throughout the tests. The average rotation speed was 800 rpm and this value was selected considering that the electrolyte in the industrial process has a countercurrent flow, with respect to the direction in which the strip advances, at a speed of 1 m/s and the average line speed is 0.67 m/s. Hence, tangential speed of the disk in rotation was adjusted with the addition of the electrolyte speed plus the advance speed of the steel strip: 1 m/s + 0.67 m/s = 1.67 m/s which equals to 800 rpm [8, 10]. The electrolyte used was a zinc sulfate solution with a [Zn^{+2}] concentration between 40 and 140 g/L and was prepared diluting $ZnSO_4 \cdot 7H_2O$ (Biopack, 99.9 %) with double distilled water. In all the experiments carried out in this work the pH was adjusted to 2, measured at 20 °C, adding sulfuric acid (Anedra, 98 %). The temperature of the solution was controlled between 40 and 70 °C using a Frigomix 1495 thermostatic bath and a double wall cell. CD was varied between 20 and 65 A/dm^2 with a DC power supply (FullEnergy HY3020 model) when galvanostatic deposition was carried out. In potentiostatic deposition experiments, the cathode potential was measured against a saturated calomel electrode (SCE) with a Luggin capillary located at $\approx$0.3–0.5 mm from the washer edge (Fig. 1). Ohmic drop compensation was estimated, as described elsewhere [18], in order to convert the measured potentials into overpotential values. These are reported as positive throughout this work for simplicity, so they must be considered as the absolute value of the measured quantity. This ohmic compensated overpotential (η) was varied from 3.8 to 5.3 V and the current was recorded with a high precision digital multimeter (Pro'sKit MT-1860) connected in series with the power supply and the zinc anode. A summary of the operating parameters is presented in Table 1.

Some washers were weighed before and after Zn deposition at different experimental conditions and the current efficiency was estimated to be practically 100 % in all the cases. The latter implies that hydrogen evolution is negligible at the working pH, so it has no effect on dendrites formation during Zn electrodeposition at the conditions under study. Anodic process involves only Zn oxidation to Zn^{+2} ions and the larger anodic area relative to the cathodic one (3:1) prevents any anodic polarization. Thus, no secondary reactions at the cathode nor at the anode had to be considered for the discussion of the results.

Polarization curves were performed reading the CD at fixed η values for rotation speeds between 400 and 1200 rpm, 60 °C electrolyte temperature, 90 g/L zinc concentration. η was increased in approximately 1 V steps, holding each value for 10 s. The CD transients stabilized very rapidly and in 0.5 s, the readings were constant.

2.2 Washer edge finish

The laser cutting process produces a characteristic rough edge which does not represent the typical edge found in the steel strip along the production line [10]. Knowing the importance of strip edge quality in electrodeposition, the edges of all the samples were standardized by a systematic reproducible procedure. One set of samples (G80) were rotated at 600 rpm and their edges were grinded using 80-grit sandpaper during 1 min at constant pressure. The edges of a second set of washers (G600) were grinded for 1 min with 180-grit, 1 min with 320-grit and finally 1 min with 600-grit sandpapers. A hard plastic block was used as a backup for the sandpapers. New sandpapers were used for each sample. Two finishes were obtained with optical microscopy (OM) images similar to the OM images of industrial samples [10]. As the roughness of the washer edge is very difficult to measure, the finishing procedures were applied to the flat portion of a washer and its roughness was measured. This was done using a Homer T1000 profilometer with a sweep length of 4.8 mm and a cut off length of 0.8 mm. For the G80 procedure, an average roughness value of 0.80 μm was obtained and for the G600 this value was 0.24 μm. The roughness of the industrial steel strip is in the range of 0.50–1.50 μm, indicating that G600 samples are smoother and G80 washers are within the practical case.

2.3 Characterization of Zn deposits

Zn deposits were evaluated by OM using a USB digital microscope (Digi View 200X) and by scanning electron microscopy (SEM) with a Quanta200 FEI equip (Tungsten filament source). The dendrites length was measured from OMs of washer edges using an image analysis freeware (Piximetre 5.4). A number of 50 dendrites, chosen at random, were measured and the mean of the lengths distribution is reported.

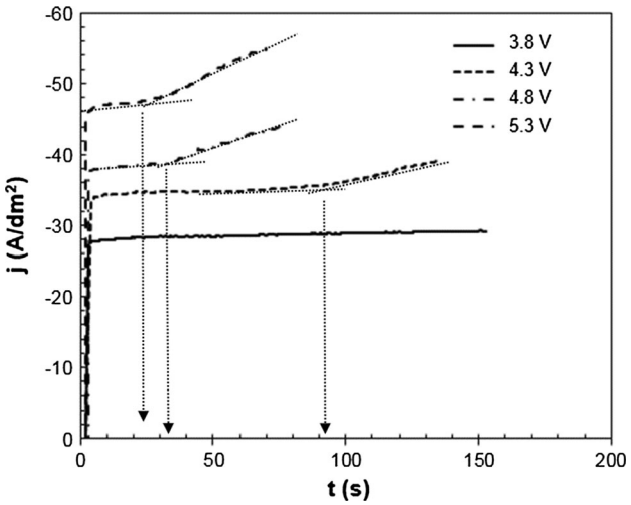

Fig. 2 Potentiostatic CD transients for G80 washers at 800 rpm, 50 °C, 90 g/L [Zn^{+2}] for several overpotentials (η)

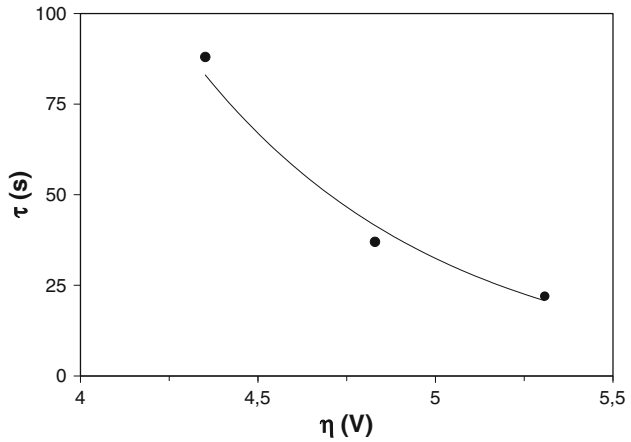

Fig. 3 τ as a function of η for G80 washers at 800 rpm, 50 °C, 90 g/L [Zn^{+2}]

3 Results

3.1 Potentiostatic depositions

During potentiostatic deposition of zinc on G80 washers, CD was registered. Figure 2 shows the time dependence of CD at several overpotentials. It can be seen that, except for 3.8 V, all the CD curves present a slope change at a particular time called "induction time" (τ), which has been described elsewhere [14, 16, 17]. The dependence of τ with

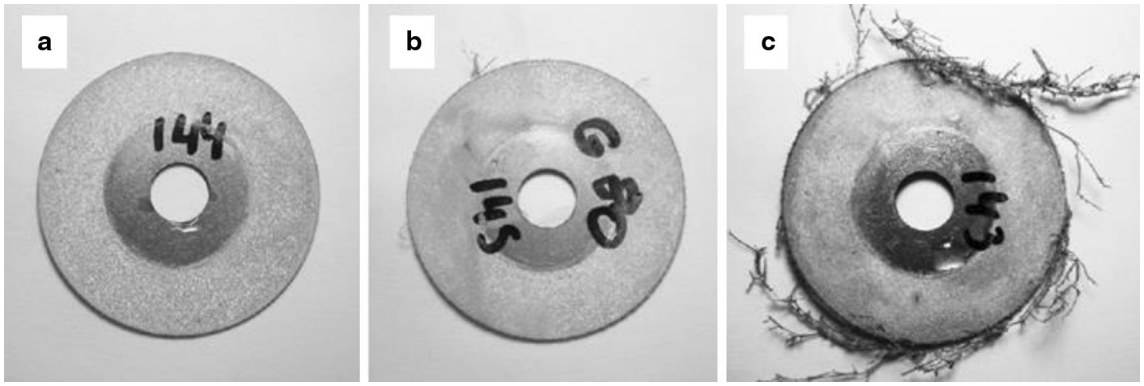

Fig. 4 OM images of Zn deposits on G80 washers obtained at **a** 20 s, **b** 40 s and **c** 120 s. The deposition conditions were: 800 rpm, $T = 50$ °C and 90 g/L [Zn^{+2}]

η, shown in Fig. 3, is exponential as was postulated by Bockris et al. [17]. for Zn electrodeposition in an alkaline electrolyte. More trials were done for 3.8 V $< \eta <$4.3 V but no τ was detected for deposition times (t_d) as long as 720 s. These long times have no practical meaning and these experiments were discarded. It was concluded that 4.3 V is the minimum η value that produces dendritic growth in this particular application.

Potentiostatic zinc deposits obtained at $\eta = 5.3$ V ($\tau = 28$ s) were characterized with OM for t_d lower and higher than τ. The OM image of zinc deposits for $t_d = 20$ s in Fig. 4a, shows that no dendrites were formed. For $t_d = 40$ s few dendrites have grown on the washer edge (Fig. 4b). Finally, for $t_d = 120$ s ($t_d \gg \tau$), a high density of long zinc dendrites can be appreciated. This behavior is consistent with the induction time concept.

3.2 Polarization curves

Figure 5 shows the potentiostatic polarization curves for the RWE at 400, 800 and 1200 rpm for G80 washers. It is clear that the dependence of CD with overpotential is linear for 1200 rpm and 800 rpm in the entire overpotential region studied. This behavior is characteristic of ohmic control [19]. For $\omega = 400$ rpm CDs are higher and the dependence is linear only at the lower η region, and it growths more rapidly with the increase in cathodic polarization. This abrupt change in CD has been widely studied for different electrode geometries and fluid dynamic conditions, and is usually attributed to the onset of dendritic growth [19]. It is also evident that the CDs are higher when ω decreases, for the same η. This can be explained if one assumes that the coarsening of the coating is more pronounced for the lower ω values due to the higher thickness of the turbulent limiting diffusion layer [20]. This will be confirmed later in this work.

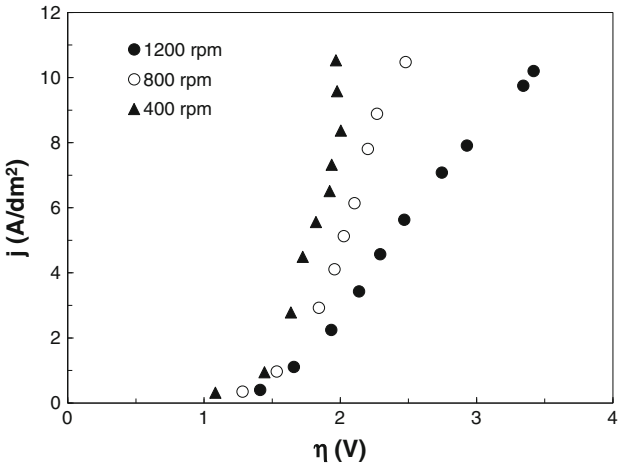

Fig. 5 Potentiostatic polarization curves for G80 washers

3.3 Initial stages of dendrite formation

In order to understand the initial steps of dendrite growth under fluid dynamic conditions similar to industrial plating lines and to know their precise location on the washer edge, deposits were obtained on G600 washers for very short deposition times. The deposition parameters were fixed at 38.6 A/dm^2, 60 °C, 800 rpm and 90 g/L [Zn^{+2}].Under these experimental conditions $\tau = 20$ s (not shown). Figure 6 shows the SEM images of one of the corners of the washer's edges. For $t_d = 2$ s the zinc coating is smooth and well distributed over the flat side and the edges of the washers (Fig. 6a). Figure 6b and c shows that bigger zinc crystals start to grow at the corner of the washer edges for $t_d = 5$ and 10 s respectively. From this series of SEM images it is clear that zinc crystals grow faster at the very right angle of the corner, where the CD lines concentrate [2, 21, 22].From Fig. 6d it can be confirmed that at $t_d = \tau$ the dendrite precursors have already formed supporting the induction time theory. It is also clear that these precursors are quite different

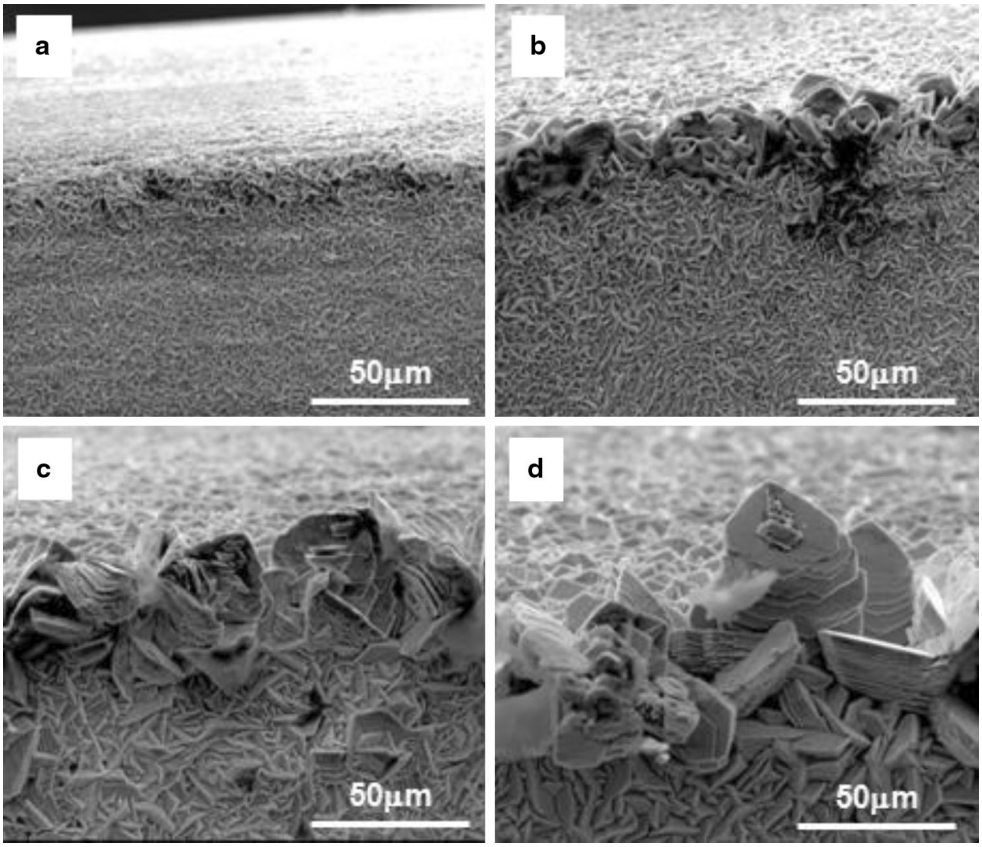

Fig. 6 SEM images of washer edge at ×2000 for different t_d values; **a** 2 s, **b** 5 s, **c** 10 s and **d** 20 s

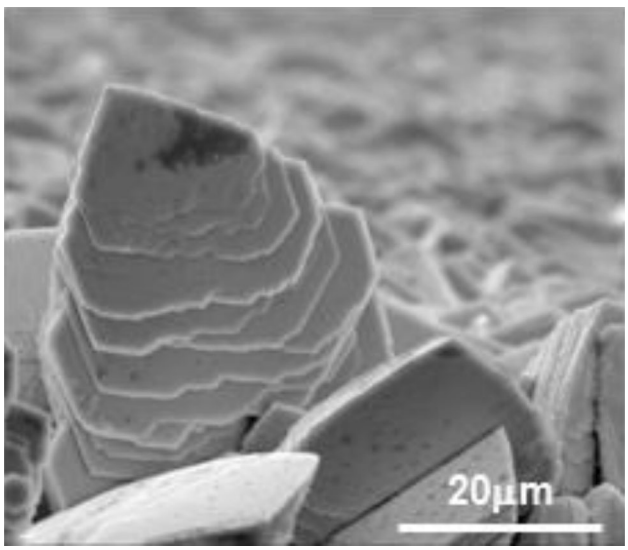

Fig. 7 SEM image of dendrite tip for $t_d = 20$ s (same sample shown in Fig. 6**d**)

from the zinc crystals deposited on the flat part of the steel substrate. From these images it can be inferred that the initiation of dendritic growth is the unavoidable result of a continuous electrochemical process.

In Fig. 7, a detail of a dendrite tip is shown. It can be seen that it is very faceted, which is characteristic of activation controlled metal deposition growth as described elsewhere [23–25].

3.4 Zinc concentration effect

Zinc was deposited galvanostatically at 40, 90 and 140 g/L of Zn^{+2} on G600 and G80 washers for $t_d = 30$ s, at 50 °C, $\omega = 800$ rpm and 49 A/dm^2. The OM images in Fig. 8a and c show that for $[Zn^{+2}] = 40$ g/L very long Zn dendrites were formed on the corners of the washer's edges. When $[Zn^{+2}]$ is increased to 90 g/L this long crystals disappeared for G600 finish (not shown) and are almost completely reduced for G80 washers (not shown). When $[Zn^{+2}]$ reaches 140 g/L the dendrites were absent for both roughnesses (Fig. 8b, d). This behavior is compatible with the activated controlled growth of tip dendrites during diffusion controlled or ohmic-diffusion controlled electrodeposition of metals [17].

According to Pavlovic et al. [26] the minimum overpotential at which dendritic growth is possible (η_i) can be expressed as:

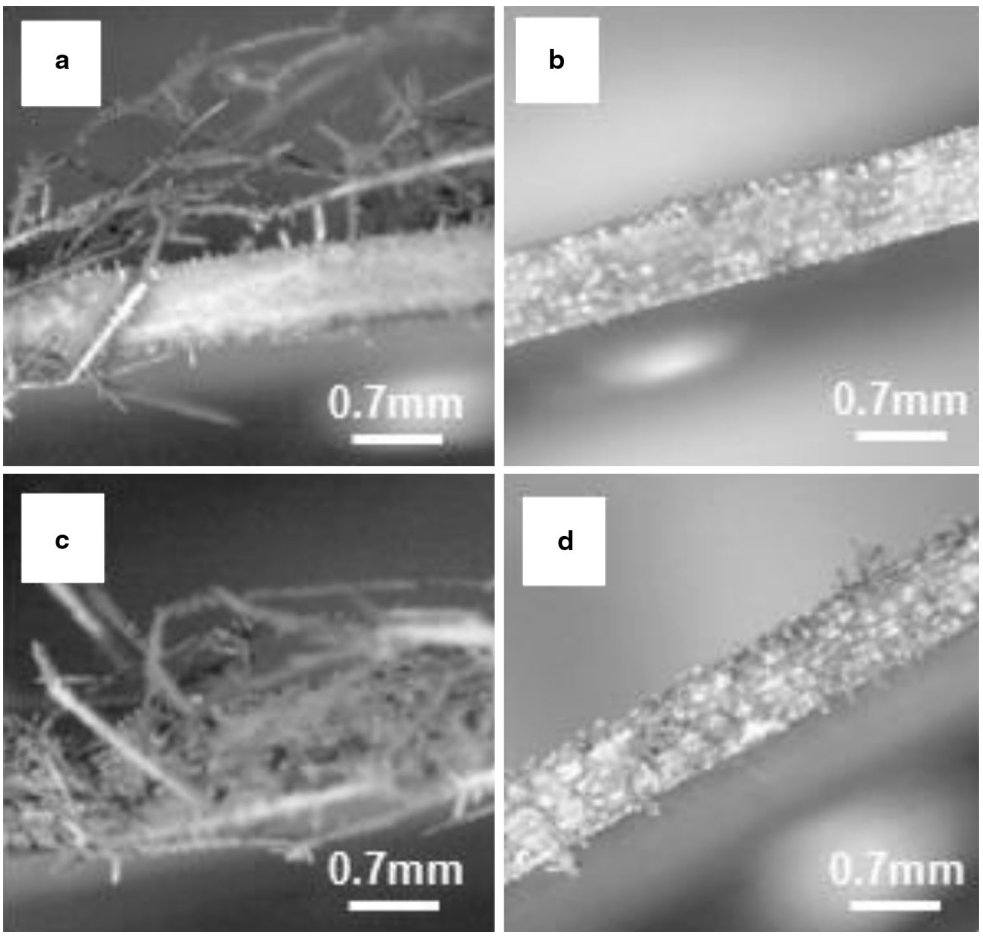

Fig. 8 OM images of Zn deposits on G600 (**a**, **b**) and G80 (**c**, **d**) washers. $[Zn^{+2}] = 40$ g/L (**a**, **c**), and 140 g/L (**b**, **d**)

$$\eta_i = \eta_0 \ln k \frac{J_L}{J_0} \tag{1}$$

where $k \geq 1$ and its value depends on the physical model used to derive the equation of η_i vs (j_L/j_0), η_0 is the slope of the Tafel line, j_0 is the exchange CD and j_L is the limiting CD. It is known that, in general, under the same hydrodynamic regime,

$$j_L \propto C_0 \tag{2}$$

where C_0 is the bulk concentration of Zn^{+2}. j_0 is also dependent on C_0 through,

$$j_0 \propto C_0^n \tag{3}$$

where n is a positive real number lower than one. From (1), (2) and (3) it follows that a system like the RWE would have a positive dependence of η_i with C_0,

$$\eta_i \propto \ln C_0^{(1-n)} \tag{4}$$

This effect is clearly seen on the OM images of deposits shown in Fig. 8.

3.5 Rotation speed of the cathode

If the $[Zn^{+2}]$ is kept constant at 90 g/L and the hydrodynamic conditions are modified, based on Eq. (1) it is reasonable to expect a dependence of η_i with j_L,

$$\eta_i \propto \ln j_L \tag{5}$$

In the case of a rotating disk electrode and a rotating cylinder electrode, j_L has defined dependences with ω [3, 20, 27] which have in common:

$$j_L \propto w^a \tag{6}$$

where a is a positive number lower than one. Although j_L vs ω functionality has not been determined yet, Blurton and Riddiford [28] studies have shown that the hydrodynamic around an electrode with a configuration like the RWE, should be similar to that found in a rotating disc electrode (RDE) configuration. Then, it is expected that j_L at the RWE would have a similar functionality with ω, which leads to the following relationship between the η_i and the rotation speed.

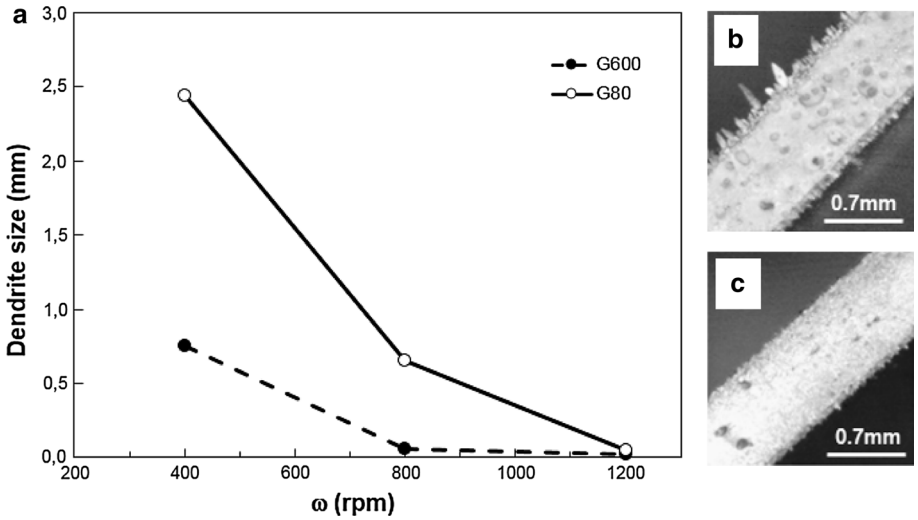

Fig. 9 Effect of ω on the dendritic growth; **a** Dendrite size versus ω, **b** image of washer edge at 400 rpm (G600), **c** image of washer edge at 1200 rpm (G600)

$$\eta_i \propto \ln w^a \tag{7}$$

It is worth noting that the value of a may be different from that of the RDE ($a = 0.5$), especially because it is impossible to neglect the edge effects at the RWE, which causes deviations from Levich's equation [29].

Deposits were obtained for G80 and G600 finishes at 60 °C and CD = 49 A/dm^2 ($t_d = 30$ s). The rotation speed ω was adjusted to 400 rpm, 800 and 1200 rpm to verify the aforementioned relationship. The curves in Fig. 9a show that dendrites average length increases with decreasing ω. This supports the mathematical relation previously derived (Eq. 7). OM images of Fig. 9b, c show, as an example, the effect of ω on dendritic growth for G600 washers. In the case of G80 washers the dendrites are very long, growing several millimeters far from the washer edge (not shown) at 400 rpm. In contrast, for higher ω values the dendrites are very short or absent. These results are consistent with the polarization curves behavior reported in Sect. 3.2.

3.6 Electrolyte temperature

According to the general model of disperse and dendritic metal electrodeposits formation derived by Popov and co-workers [17, 21], for very fast processes ($j_0/j_L \gg 1$), the critical overpotential for instantaneous dendritic growth (η_c) can be expressed as,

$$\eta_c = \frac{RT}{nF}\frac{J_L}{J_0} * (\delta/h)^{\gamma} \tag{8}$$

Where δ stands for the thickness of the diffusion layer, T is the temperature, h is the substrate protrusion height and $\gamma =$ is a parameter used in the equation of the general polarization curve [2].For the case of zinc electrodeposition in acid sulfate electrolyte, j_0 is very high and j_L/j_0 ratio is not expected to vary considerable with the temperature. Considering this, it follows from Eq. 8 that under the same fluid dynamic conditions and Zn^{+2} concentration, η_c should increase when raising electrolyte's temperature. Curves in Fig. 10a show that dendrite length decreases considerably with increasing temperature, confirming the preceding statement. As an example, OM images of zinc deposits obtained on G600 washers at $[Zn^{+2}] = 90$ g/L, $\omega = 800$ rpm, $t_d = 30$ s, CD = 49 A/dm^2, for 40 and 70 °C are shown in Fig. 10b, c. It is evident that the size and the number of the dendrites on the edge of the washers diminish when the temperature is increased from 40 to 70 °C. These results also show that dendritic growth is very sensitive to surface roughness.

3.7 Surface roughness of the cathode

In the steel making industry, it is well known that when the edge of the steel strip has quality defects, such as burr generated during side trimming, or they are mechanically damaged in other production step before the electrogalvanizing process, dendrites can grow easily during electrodeposition. In order to understand how the edge roughness influences dendrite growth, the following relation has to be considered,

$$h = h_0 \exp\left(\frac{VDC_0}{\delta^2} t_d\right) \tag{9}$$

which describes the variation of surface protrusions height with plating time [17, 30].Where h_0 is the initial protrusion height of the cathode surface, V is the molar volume of the metal and D is the diffusion coefficient of Zn^{+2} ions. Considering Eq. 8 together with Eq. 9, it can be seen that at high h_0, related to roughness, the overpotential at which instantaneous dendrite formation can occur will be lower.

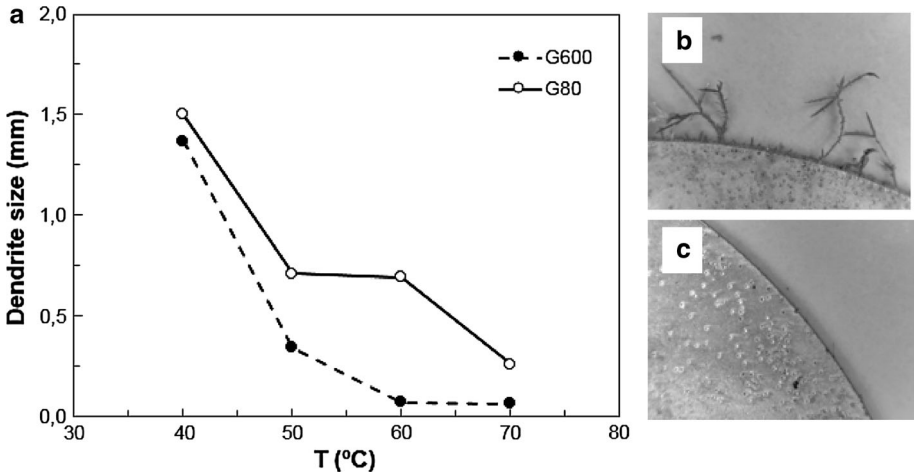

Fig. 10 Effect of temperature on dendritic growth; **a** Dendrite size versus T, **b** image of washer at 40 °C (G600), **c** image of washer at 70 °C (G600)

This means that at higher substrate roughness there will be a higher probability to have dendritic growth at lower overpotential or lower CD. Some evidence of this effect was shown in Figs. 8,9 and 10 where it is easy to see the difference between the G600 and G80 finishes on the initiation of the dendritic growth on the washer edges. Some initial results on this topic were also presented elsewhere [8–11]. Furthermore, an increase in h_0 will lead to a reduction of the induction time when the temperature and the CD or η are kept constant.

4 Conclusions

The results obtained in this work showed that dendritic growth is a complex process which depends on several electrodeposition parameters. Among them, the electrochemical potential at which zinc deposition is carried out greatly influences dendrite formation. Moreover, it is possible to suppress this kind of growth by working at sufficiently low overpotentials (below η_i), which is in complete agreement with the commonly accepted theory. The latter also accounts for the effects on the induction time and dendrite growth observed when the temperature, rotation speed and $[Zn^{+2}]$ are modified. It was found that an increase in any of these variables increases the induction time, thus reducing dendrites size when deposition time t_d is kept constant. Finally, surface roughness proved to play a major role in promoting dendritic growth. This could explain the fact that during steel strip electroplating, dendrites form at the strip edge where singular points with high roughness can be found due to side trimming defects.

The experimental setup developed in this work was suitable to study dendritic growth on non-stationary conditions. This allowed for the validation of Popov et al. theory on conditions that, to our knowledge, have not been investigated until now. In addition, the RWE reproduced well the experimental conditions found in a steel strip zinc plating line, being a powerful tool to understand processes taking place at an industrial scale. Further research on dendrite formation during electrodeposition of other metals should be carried in order to confirm the versatility of the RWE setup.

Acknowledgments The authors would like to thank the Comisión de Investigaciones Científicas de la Provincia de Buenos Aires (CICPBA), Consejo Nacional de Investigaciones Científicas y Técnicas (CONICET) and Universidad Nacional de La Plata (UNLP) for their financial support to this research.

References

1. Gamburg YD, Zangari G (2011) Theory and practice of metal electrodeposition. © Springer Science + Business Media, New York, pp 143–169. doi:10.1007/978-1-4419-9669-5
2. Ibl N (1983) Current distribution. In: Yeager E, Bockris IO'M, Conway BE, Sarangapani S (eds) Comprehensive treatise of electrochemistry, vol 6. Plenum Press, New York, pp 239–311
3. Newman JS (1991) Electrochemical systems, 2nd edn. Prentice Hall Inc., New Jersey
4. Plating and Electroplating (1994) In: Surface Engineering, vol 5. ASM International, ASM Handbook, p 257
5. Paunovic M, Schlesinger M (2006) Fundamentals of electrochemical deposition. Wiley, The Electrochemical Society Series
6. Banik SJ, Akolkar R (2013) Suppressing dendrite growth during zinc electrodeposition by PEG-200 Additive. J Electrochem Soc 160(11):D519–D523. doi:10.1149/2.040311jes
7. Kruglikov SS, Kudryavtsev NT, Vorobiova GF, Antonov AY (1965) On the mechanims of levelling by addition agents in electrodeposition of metals. Electrochim Acta 10:253–261
8. Bengoa LN, Bruno S, Lazzarino HA, Seré PR, Egli WA (2013) Generación de dendritas en borde de chapa durante el electrocincado en medio ácido. Paper presented at the 13er Congreso Internacional en Ciencia y Tecnología de Metalurgia y Materiales 2013, Puerto Iguazú, Argentina
9. Bengoa LN, Seré PR, Egli WA (2014) Influencia de la concentración de cinc en la formación de dendritas de borde en el electrocincado de chapas de acero. Paper presented at the XXI

Congreso de la Sociedad Iberoamericana de Electroquímica, La Serena, Chile
10. Bengoa LN, Bruno S, Lazzarino HA, Seré PR, Egli WA (2014) Dendritic zinc growth on the edges of flat steel strip during electro galvanizing. Proc Mater Sci [Epub ahead of print]
11. Egli WA, Seré PR, Bengoa LN (2013) Formación de dendritas de cinc en electrocincado en medio ácido. Final Report, Leg. No 15282/13. Centro de Investigación y Desarrollo en Tecnologías de Pinturas (CIDEPINT)
12. Zubimendi JL, Baieli C, Egli W, Chara MR, Andreasen G, Schilardi P, Salvarezza R, Marchiano S (1996) The influence of operating conditions on the morphology of tin electrodeposits and tinplate quality. In: 6th Tinplate conference, London, 1996
13. Wranglén G (1960) Dendrites and growth layers in the electrocrystallization of metals. Electrochim Acta 2:130–146
14. Diggle JW, Despić AR, Bockris JOM (1969) The mechanism of the dendritic electrocrystallization of zinc. J Electrochem Soc 116(11):1503–1514
15. Popov KI, Maksimović MD, Trnjancev JD, Pavlović MG (1981) Dendritic electrocrystallization and the mechanism of powder formation in the potentiostatic deposition of metals. J Appl Electrochem 11(239–246):239–246
16. Popov KI, Djukić LM, Pavlović MG, Maksimović MD (1979) The critical overpotential for copper dendrite formation. J Appl Electrochem 9:527–531
17. Popov KI, Nikolic ND (2012) General theory of disperse metal electrodeposits formation. In: Djokić SS (ed) Electrochemical production of metal powders. Modern aspects of electrochemistry, vol 54. Springer Science + Business Media, New York, pp 1–62
18. Vetter KJ (1967) The theory of overvoltage. In: Bruckenstein S, Howard B (eds) Electrochemical kinetics. Theoretical and experimental aspects. Academic Press, New York, pp 392–395
19. Popov KI, Živković PM, Krstić SB, Nikolić ND (2009) Polarization curves in the ohmic controlled electrodeposition of metals. Electrochim Acta 54(10):2924–2931. doi:10.1016/j.electacta.2008.11.004
20. Bard AJ, Faulkner LR (2001) Electrochemical methods. Fundamental and applications, 2nd edn. Wiley, New York
21. Popov KI, Djokić SS, Grgur BN (2002) Surface morphology of metal electrodeposits. Fundamental aspects of electrometallurgy. Kluwer Academic/Plenum Publishers, New York, pp 29–100
22. Despić AR, Popov KI (1972) Transport control deposition and dissolution of metals. In: Conway BE, Bockris JOM (eds) Modern aspects of electrochemistry, vol 7. Butterworths, London, pp 304–310
23. Nikolić ND, Popov KI, Živković PM, Branković G (2013) A new insight into the mechanism of lead electrodeposition: ohmic-diffusion control of the electrodeposition process. J Electroanal Chem 691:66–76. doi:10.1016/j.jelechem.2012.12.011
24. Nikolić ND, Branković G, Lačnjevac UČ (2012) Formation of two-dimensional (2D) lead dendrites by application of different regimes of electrolysis. J Solid State Electrochem 16:2121–2126. doi:10.1007/s10008-011-1626-y
25. Jović VD, Nikolić ND, Lačnjevac UČ, Jović BM, Popov KI (2012) Morphology of different electrodeposited pure metal powders. In: Djokić SS (ed) Electrochemical production of metal powders. Modern aspects of electrochemistry, vol 54. Springer Science + Business Media, New York, pp 63–123
26. Pavlović MG, Kindlová S, Rousar I (1992) The initiation of dendritic growth of electrodeposited copper on a rotating disc electrode with changing copper concentration and diffusion layer thickness. Electrochim Acta 37(1):23–27
27. Gabe DR, Wilcox GD, Gonzalez-Garcia J, Walsh FC (1998) The rotating cylinder electrode: its continued development and application. J Appl Electrochem 28:759–780
28. Blurton KF, Riddiford AC (1965) Shapes of practical rotating disc electrodes. J Electroanal Chem 10:457–464
29. Levich VG (1962) Physicochemical hydrodynamics. Prentice-Hall, Englewood Cliffs
30. Popov KI, Pavlovic MG, Maksimovic MD (1982) Comparison of the critical conditions for initiation of dendritic growth and powder formation in potentiostatic and galvanostatic copper electrodeposition. J Appl Electrochem 12:525–531